Protostars and pre-main sequence evolution

1. Timescales
2. Early growth and collapse
3. Dust envelope
4. Stellar structure
    - I. Mass-radius relation
    - II. Deuterium burning
    - III. Lithium destruction
    - IV. Hydrogen ignition
5. Magnetospheric accretion
    - I. Theory
    - II. Observations
6. Evolution in the HR diagram
    - I. Birthline
    - II. Hayashi tracks
7. PMS classification
    - I. T Tauri stars
    - II. Weak line T Tauri stars
    - III. FU Orionis stars
    - IV. Herbig AeBe stars

Definitions

- A protostar is the object that forms in the center of a collapsing cloud, before it becomes (optically) visible.
- A pre-main sequence star is optically visible and has no central hydrogen burning
- As soon as hydrogen burning starts, the object is called a star (main sequence star).

Timescales

Free-fall timescale: $t_{\rm ff} = \sqrt{\frac{3\pi}{32 G\rho}} \approx \sqrt{\frac{1}{G\rho}}$

Kelvin-Helmholtz timescale: $t_{\rm KH} = \frac{U_{\rm grav}}{L_*} = \frac{3}{5}\frac{GM_*^2}{R_* L_*}$

Accretion timescale: $t_{\rm acc} = \frac{M_{\rm core}}{\dot{M}}$

t_{ff} « $t_{\rm KH}$ or $t_{\rm acc}$ the free-fall timescale is much shorter than the other two

Timescales

We can distinguish two cases:

$t_{\mathrm{KH}} \gg t_{\mathrm{acc}}$

Stellar interior does not adjust thermally as new matter get piled onto the top. Luminosity is generated at the surface by accretion shock. This is the 'protostellar phase'.

$t_{\mathrm{KH}} \ll t_{\mathrm{acc}}$

Star evolves toward main sequence on a thermal timescale, the contraction is slow; luminosity is generated by contraction. This is the 'pre-main sequence phase'.

Using $\dot{M} \sim \frac{c_s^3}{G} \sim 1.6 \times 10^{-6}\ \mathrm{M}_\odot\ \mathrm{yr}^{-1}$ (Shu inside-out collapse),

the timescale for forming a 1 $M_\odot$ star from a 10 K cloud is 6.3 x 10^5 yr.

The protostar

Isothermal approximation no longer valid, because the central core becomes optically thick to its own radiation

- The central temperature rises steadily
- The internal pressure stabilizes the core
- The core grows through accretion until it reaches R~5 AU and M~5x10^{-2} $M_\odot$

The protostar

From the virial theorem, we can derive an estimate of the core temperature

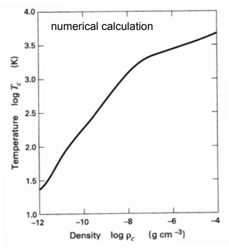

$$\begin{aligned} U_{\mathrm{grav}} &= -\frac{3}{5}\frac{GM_*^2}{R_*} \\ = -2U_{\mathrm{therm}} &= -2\frac{3}{2}\frac{kTM_*}{\mu m_{\mathrm{H}}} \end{aligned}$$

$$\Downarrow$$

$$T = \frac{m}{5k}\frac{GM_*}{R_*} \approx 520\ K \left(\frac{M_*}{5 \times 10^{-2}\ \mathrm{M}_\odot}\right)\left(\frac{R_*}{5\ \mathrm{AU}}\right)^{-1}$$

The H_2 thermostat

At temperatures >2000 K, collisions can dissociate H_2

$\Delta E(H_2 \text{ diss}) = -4.48$ eV

E_{kin} = 0.74 eV

=> most of the gravitational contraction energy can be absorbed through the dissociation of a small fraction of the total H_2

The temperature rise of the core becomes more moderate.

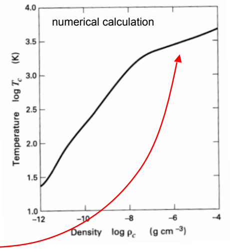

Central zone of atomic H spreads outward until the adiabatic index γ is pushed below 4/3 => unstable configuration, second collapse phase

The second core

During the second collapse, as ρ reaches ~10^{-2} g/cm^3 hydrogen can be ionized => γ again pushed above 4/3

=> second stable core which reaches 0.01 - 0.02 $M_\odot$ in less than 100 yr

The protostar grows to its final mass during the 'protostellar phase', where $t_{KH} \gg t_{acc}$

What is the protostars maximum size and luminosity?

The protostar

Using the virial theorem $U_{\rm therm} = -1/2\, U_{\rm grav}$

energy conservation yields: $-\frac{1}{2}\frac{3}{5}\frac{GM_*^2}{R_*} + E_{\rm int} + L_{\rm rad}t = 0$

$L_{\rm rad}$ - energy radiated away over a timescale t

$E_{\rm int}$ - internal energy of the gas

$E_{\rm int}$ at $t = 0$ is zero (very large cold cloud), and later given by H_2 dissociation (4.48 eV) and H,He ionization (13.6, 75 eV)

$$\Delta E_{\rm int} = \frac{XM_*}{m_{\rm H}}\left[\frac{\Delta E_{\rm diss}({\rm H_2})}{2} + \Delta E_{\rm ion}({\rm H})\right] + \frac{YM_*\Delta E_{\rm ion}({\rm He})}{4m_{\rm H}}$$

where X is the mass fraction of hydrogen and Y that of helium

The protostar

Energy conservation yields: $-\frac{1}{2}\frac{3}{5}\frac{GM_*^2}{R_*} + E_{\rm int} + \cancel{L_{\rm rad}} t = 0$

ignore $L_{\rm rad}$

and hence $\boxed{R_{\rm max} = \frac{3}{10}\frac{GM_*^2}{\Delta E_{\rm int}} = 36\ R_\odot \left(\frac{M_*}{{\rm M}_\odot}\right)}$

Observed radii of pre-main sequence stars (T Tauri stars) are ~1 order of magnitude smaller

=> $\Delta E_{\rm int} < -\frac{1}{2}\frac{3}{5}\frac{GM_*^2}{R_*}$ and we can neglect it

Then we obtain an estimate for the luminosity $L_{\rm acc} = \frac{3}{10}\frac{GM_*}{R_*}\dot{M}$

$$\boxed{L_{\rm acc} \approx 18\ L_\odot \left(\frac{\dot{M}}{10^{-5}\ {\rm M}_\odot\ {\rm yr}^{-1}}\right)\left(\frac{M_*}{{\rm M}_\odot}\right)\left(\frac{R_*}{5{\rm R}_\odot}\right)^{-1}}$$

The protostar

$$\boxed{L_{\rm acc} \approx 18\ L_\odot \left(\frac{\dot{M}}{10^{-5}\ {\rm M}_\odot\ {\rm yr}^{-1}}\right)\left(\frac{M_*}{{\rm M}_\odot}\right)\left(\frac{R_*}{5{\rm R}_\odot}\right)^{-1}}$$

What do we learn from this?

Radiative energy loss directly connected to contraction

$$\begin{aligned} L_* &= 4\pi R_*^2 \sigma T_*^4 \\ T_* &= \left(\frac{L_*}{4\pi\sigma R_*^2}\right)^{1/4} \approx \text{constant} \quad \text{(assumption)} \\ L_* &= L_0 \frac{R_*^2}{R_0^2} \\ L_* &= L_0 \left(\frac{7}{3}\frac{tL_0R_0}{GM_*^2}\right)^{-2/3} = L_0 \left(\frac{7}{5}\frac{t}{t_{\rm KH}}\right)^{-2/3} \end{aligned}$$

The rate of change in luminosity and size slows with age.

The protostar

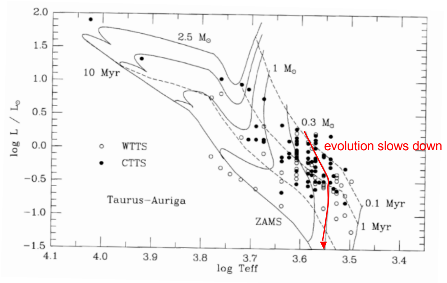

The rate of change in luminosity and size slows with age.

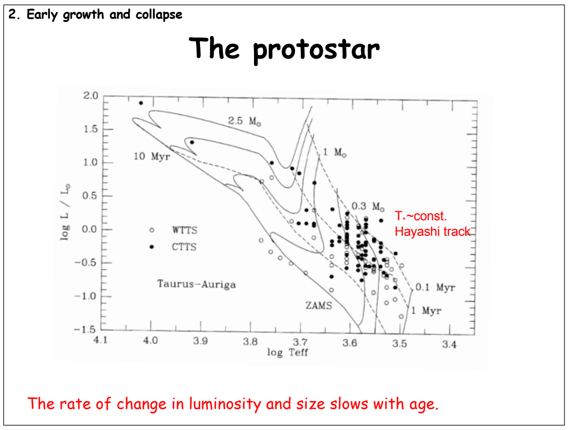

2. Early growth and collapse

The protostar

T_*~const.
Hayashi track

The rate of change in luminosity and size slows with age.

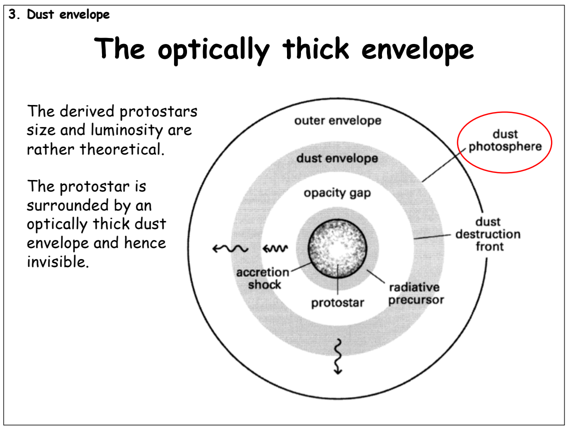

3. Dust envelope

The optically thick envelope

The derived protostars size and luminosity are rather theoretical.

The protostar is surrounded by an optically thick dust envelope and hence invisible.

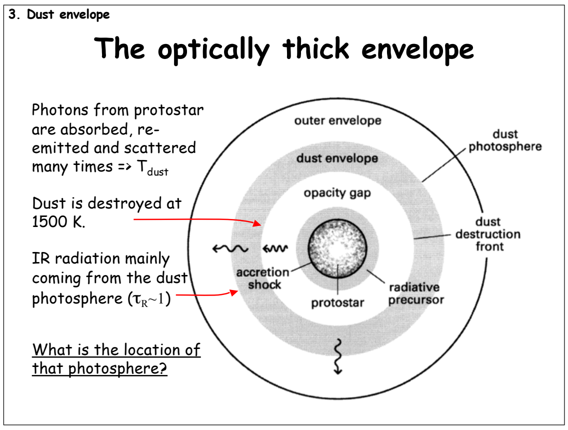

3. Dust envelope

The optically thick envelope

Photons from protostar are absorbed, re-emitted and scattered many times => T_{dust}

Dust is destroyed at 1500 K.

IR radiation mainly coming from the dust photosphere (τ_R~1)

<u>What is the location of that photosphere?</u>

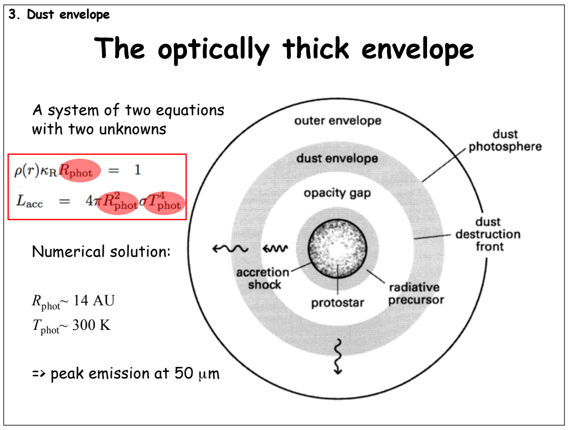

3. Dust envelope

The optically thick envelope

A system of two equations with two unknowns

$$\rho(r)\kappa_R R_{\rm phot} = 1$$
$$L_{\rm acc} = 4\pi R_{\rm phot}^2 \sigma T_{\rm phot}^4$$

Numerical solution:

$R_{\rm phot} \sim 14$ AU
$T_{\rm phot} \sim 300$ K

=> peak emission at 50 μm

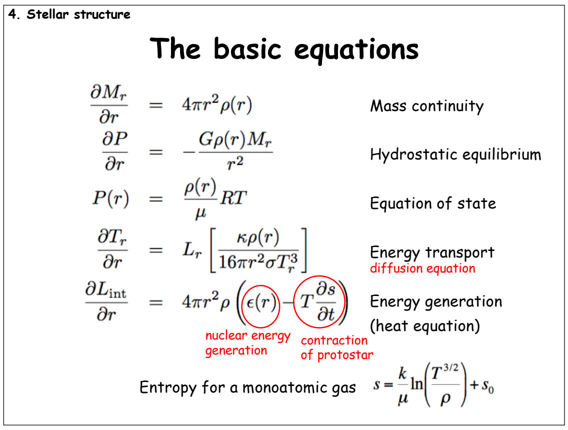

4. Stellar structure

The basic equations

$$\frac{\partial M_r}{\partial r} = 4\pi r^2 \rho(r)$$ Mass continuity

$$\frac{\partial P}{\partial r} = -\frac{G\rho(r)M_r}{r^2}$$ Hydrostatic equilibrium

$$P(r) = \frac{\rho(r)}{\mu}RT$$ Equation of state

$$\frac{\partial T_r}{\partial r} = L_r\left[\frac{\kappa\rho(r)}{16\pi r^2\sigma T_r^3}\right]$$ Energy transport

diffusion equation

$$\frac{\partial L_{\rm int}}{\partial r} = 4\pi r^2\rho\left(\underbrace{\epsilon(r)}_{\text{nuclear energy generation}} - \underbrace{T\frac{\partial s}{\partial t}}_{\text{contraction of protostar}}\right)$$ Energy generation (heat equation)

Entropy for a monoatomic gas $s = \frac{k}{\mu}\ln\left(\frac{T^{3/2}}{\rho}\right) + s_0$

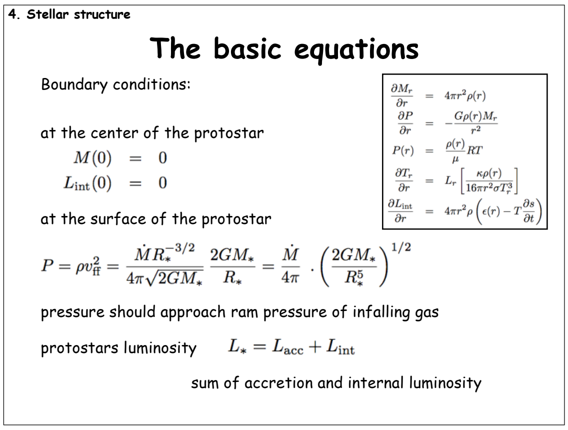

4. Stellar structure

The basic equations

Boundary conditions:

$$\frac{\partial M_r}{\partial r} = 4\pi r^2 \rho(r)$$
$$\frac{\partial P}{\partial r} = -\frac{G\rho(r)M_r}{r^2}$$
$$P(r) = \frac{\rho(r)}{\mu}RT$$
$$\frac{\partial T_r}{\partial r} = L_r\left[\frac{\kappa\rho(r)}{16\pi r^2\sigma T_r^3}\right]$$
$$\frac{\partial L_{\rm int}}{\partial r} = 4\pi r^2\rho\left(\epsilon(r) - T\frac{\partial s}{\partial t}\right)$$

at the center of the protostar

$$M(0) = 0$$
$$L_{\rm int}(0) = 0$$

at the surface of the protostar

$$P = \rho v_{\rm ff}^2 = \frac{\dot M R_*^{-3/2}}{4\pi\sqrt{2GM_*}}\,\frac{2GM_*}{R_*} = \frac{\dot M}{4\pi}\cdot\left(\frac{2GM_*}{R_*^5}\right)^{1/2}$$

pressure should approach ram pressure of infalling gas

protostars luminosity $L_* = L_{\rm acc} + L_{\rm int}$

sum of accretion and internal luminosity

The Mass-Radius relation

The system of equations needs to be solved numerically, solutions independent of initial conditions after first doubling of mass

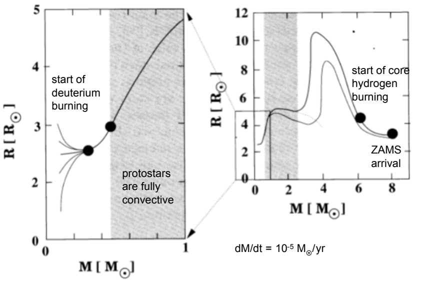

Convection

H^- is the main opacity source in the photosphere of protostars

H^- opacity highly temperature dependent (for $T < 10^4$ K) => valve that regulate the stellar surface temperature

Hayashi temperature: minimum allowed T_{eff} for a fixed M_* and R_*
=> minimum L_* (L_{min}) (HR diagram)

$\langle L_{crit} \rangle$: maximum L_*
that can be transported by radiation

$L_{min} > \langle L_{crit} \rangle$: protostar becomes fully convective

This is the case for protostars with $M_* < 2M_\odot$.

$2M_\odot < M_* < 8M_\odot$ protostars have $L_{min} < \langle L_{crit} \rangle$ and sustain a radiative core.

Convection

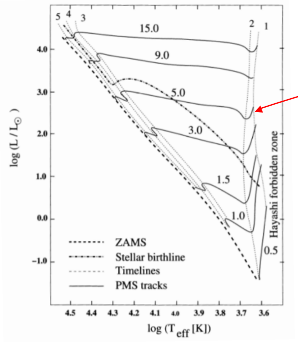

Hayashi track

Hayashi temperature:

minimum allowed T_{eff} for a fixed M_* and R_*

=> minimum L_* (L_{min})

unstable zone where the protostar cannot find a quasi-hydrostatic equilibrium

Deuterium burning

10^6 K: $^2D + ^1H \rightarrow ^3He + \gamma$

- Mass accretion provides steady supply of fuel
- Energy generation through D fusion drives convection
- Mixing of new fuel to the center
- keeps T of core very stable

=> D fusion regulates Mass-Radius relation

$L_D \sim 12\ L_\odot\ (M_{acc}/10^{-5}\ M_\odot/yr)$

However, often dM/dt not enough to keep up with consumption

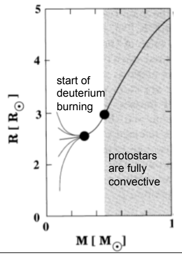

Lithium destruction

2.5 10^6 K: $^7Li + ^1H \rightarrow ^4He + ^4He$

Stars smaller than 0.9 $M_\odot$ are fully convective and quickly destroy entire ^7Li reservoir.

More massive stars cease to be fully convective before entire ^7Li is destroyed.

=> Observations of Li in pre-main sequence stars are a powerful test of pre-main sequence stellar structure and evolution models.

Hydrogen ignition

Once D fusion cease in the core, protostar collapses further until T_c large enough to start hydrogen burning.

10^7 K:

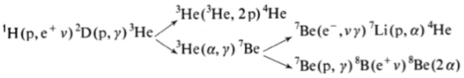

$$^1H(p,e^+\nu)^2D(p,\gamma)^3He \begin{cases} ^3He(^3He,2p)^4He \\ ^3He(\alpha,\gamma)^7Be \begin{cases} ^7Be(e^-,\nu\gamma)^7Li(p,\alpha)^4He \\ ^7Be(p,\gamma)^8B(e^+\nu)^8Be(2\alpha) \end{cases} \end{cases}$$

1.5 10^7 K: CNO cycle (C, N, O conversion into ^{14}N)

The star has reached the ZAMS.

Theory

Accretion drives the protostellar structure and evolution !

How does accretion work ?

And how large is dM/dt ?

Initial phase: accretion occurs through the envelope onto the core (very short phase)

Later phase: accretion occurs through the disk onto the protostar

Let’s briefly look at the disk accretion.

Theory

Disk accretion through angular momentum transport

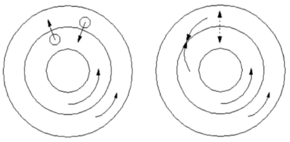

- the angular velocity is decreasing outwards.
- in the presence of friction or communication between two neighboring annuli, resulting torques try to bring them into corotation.
- gas in the outer annulus accelerates, gas in the inner annulus decelerates.
- inner annulus looses angular momentum to the outer one

Theory

Magnetospheric accretion

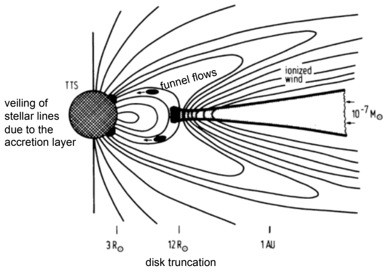

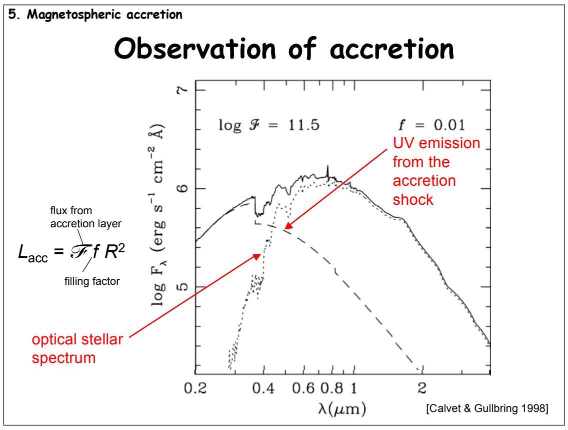

5. Magnetospheric accretion

Observation of accretion

UV emission from the accretion shock

optical stellar spectrum

flux from accretion layer

$L_{acc} = \mathcal{F} f R^2$

filling factor

[Calvet & Gullbring 1998]

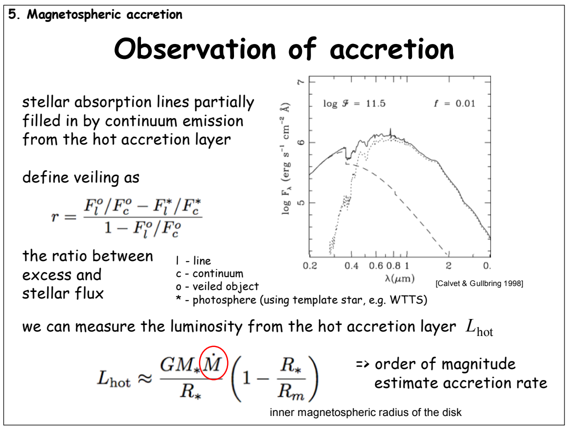

5. Magnetospheric accretion

Observation of accretion

stellar absorption lines partially filled in by continuum emission from the hot accretion layer

define veiling as

$$r = \frac{F_l^o/F_c^o - F_l^*/F_c^*}{1 - F_l^o/F_c^o}$$

the ratio between excess and stellar flux

l - line
c - continuum
o - veiled object
* - photosphere (using template star, e.g. WTTS)

[Calvet & Gullbring 1998]

we can measure the luminosity from the hot accretion layer $L_{\rm hot}$

$$L_{\rm hot} \approx \frac{G M_* \dot{M}}{R_*}\left(1 - \frac{R_*}{R_m}\right)$$

=> order of magnitude estimate accretion rate

inner magnetospheric radius of the disk

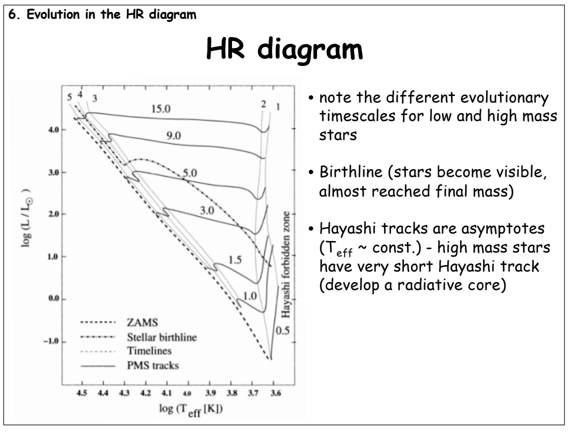

6. Evolution in the HR diagram

HR diagram

- note the different evolutionary timescales for low and high mass stars
- Birthline (stars become visible, almost reached final mass)
- Hayashi tracks are asymptotes ($T_{\rm eff}$ ~ const.) - high mass stars have very short Hayashi track (develop a radiative core)

6. Evolution in the HR diagram

HR diagram

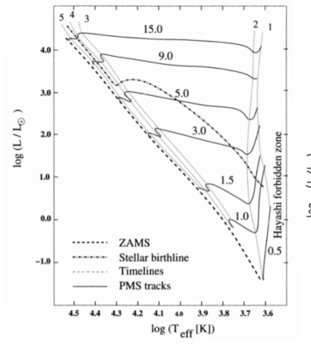

open circles CTTS (disks+accretion)
filled circles WTTS (no accretion, older)
hatched area - initial loci of PMS stars

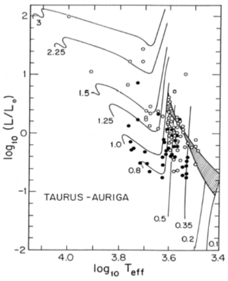

7. PMS classification

Overview

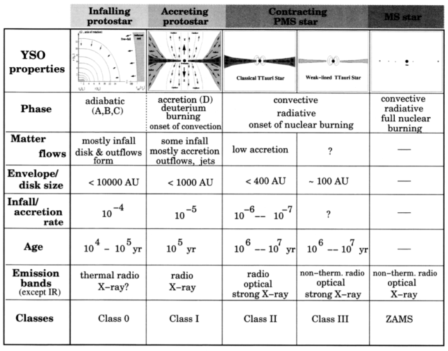

	Infalling protostar	Accreting protostar	Contracting PMS star		MS star
YSO properties			Classical TTauri Star	Weak-lined TTauri Star	
Phase	adiabatic (A,B,C)	accretion (D) deuterium burning onset of convection	convective radiative onset of nuclear burning		convective radiative full nuclear burning
Matter flows	mostly infall disk & outflows form	some infall mostly accretion outflows, jets	low accretion	?	—
Envelope/ disk size	< 10000 AU	< 1000 AU	< 400 AU	~ 100 AU	—
Infall/ accretion rate	10^{-4}	10^{-5}	10^{-6} -- 10^{-7}	?	—
Age	10^4 - 10^5 yr	10^5 yr	10^6 -- 10^7 yr	10^6 -- 10^7 yr	—
Emission bands (except IR)	thermal radio X-ray?	radio X-ray	radio optical strong X-ray	non-therm. radio optical strong X-ray	non-therm. radio optical X-ray
Classes	Class 0	Class I	Class II	Class III	ZAMS

7. PMS classification

T Tauri stars

- named after the protoype T Tau
- strong Balmer emission, association with reflection nebula and molecular clouds
- low mass stars with spectral type F-M (3000-7000 K)
- classII sources (SED peaks between 1 and 10 μm)
- large spread of disk masses: 0.0003 - 1 $M_\odot$ (median 0.01 $M_\odot$)

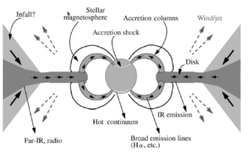

Weak line T Tauri stars

- young low mass stars associated with star forming region, but without strong Hα emission ($W_{H\alpha}$<10Å)
- Class II sources (SED shows no strong near IR excess)
- no clear accretion signatures (inner optically thick disk disappeared)

=> most likely the older counterparts of WTTS

FU Orionis stars

- spectral type F-G (6000-7000 K)
- periodic optical outbursts of several magnitudes
- rising timescale ~1 yr
- decline timescale ~50-100 yr

=> episodes of increased mass accretion (dM/dt ~ 10^{-4} $M_{\odot}$/yr), possibly related to dynamical instabilities

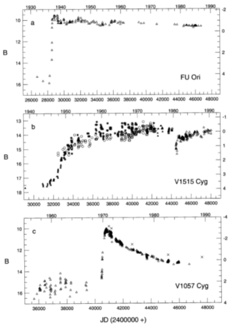

Herbig AeBe stars

- intermediate mass stars with spectral type B0-early F with emission lines (e.g. strong Hα)
- SED shows strong IR excess
- more massive counterparts of T Tauri stars
- shorter evolutionary timescales than T Tauri stars

GAS DIAGNOSTICS (1/2)

The gas associated with forming stars has densities and temperature covering a relatively large range: from 10 to few thousands Kelvins, and from 10^2 to 10^{11} cm^{-3}, respectively. Different molecular lines can be used to probe the gas in different physical conditions, namely in different regions of the protostar. The figure on the right shows the lines typically used to probe the different density and temperature regimes.

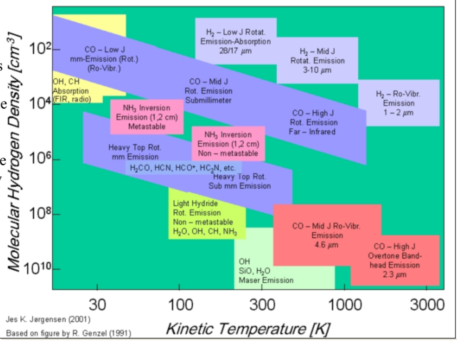

Jes K. Jørgensen (2001)
Based on figure by R. Genzel (1991)

GAS DIAGNOSTICS

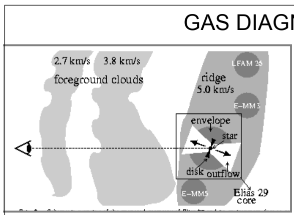

The usual situation is shown in the left figure: the protostar is embedded in the parental cloud, and perhaps other clouds lie between us and the protostar. In principle, the observed line is due to the emission from all the components in the line of sight: clouds + envelope + disk + outflow. The <u>chemical differentiation</u> and the different <u>velocities</u> associated with each component help to disentangle them.

As discussed in Chapter 5, the emergent line flux depends on the chemical abundance of the species, the gas temperature and density, the dust continuum emission, and the gas velocity field. Using appropriate molecular lines one can, hence, reconstruct the structure of the emitting region. This is a very difficult but feasible task.

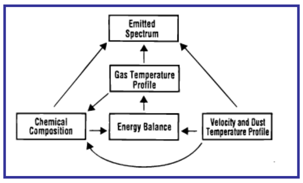

CLASS 0 SOURCES (1/3): DEFINITION

The Class 0 sources were discovered at the beginning of 90s when the large ground based telescopes like IRAM or JCMT became available. They are defined as low luminosity sources, with a proved central object, centrally condensed envelope, and whose luminosity in sub-millimeter to millimeter wavelengths L_{submm} is an important fraction of the bolometric luminosity L_{bol}: $L_{submm}/L_{bol} > 0.5\%$.
This *phenomenological* classification is meant to correspond to a physical state: the mass of the inner hidden object is lower than the mass of the surrounding envelope. In the literature, other criteria have also been proposed and used, as, for example, the bolometric temperature.
The goal of all the proposed criteria has been to identify the proprieties of protostars in the so-called ``*main accretion phase"*, i.e. the phase where the future star acquires the bulk of the mass. At present, something less than 100 protostars have been censed, all of them in clouds closer than about 400pc from the Sun.

CLASS 0 SOURCES: APPEARENCE

The prototype of the Class 0 sources is IRAS16293-2422, which lies in L1689N, a small molecular cloud in the ρ Ophiuchus complex (at ~120-160pc). The figure on the left shows a map of the H_2CO emission towards L1689N. The cloud harbors two protostars, marked by the stars in the figure: IRAS16293-2422 (at coordinates 0,0) and a colder protostars called 16293E, South-East. The figure in the right shows the same region in the N_2H^+. Note that while IRAS16293 « shines » in H_2CO, the other source, colder (and likely younger) does not. The situation is totally reversed in the N_2H^+ line, for N_2H^+ is copiously formed in cold gas.

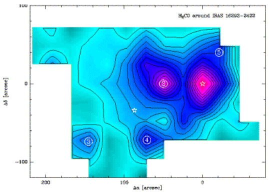

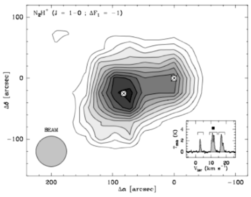

CLASS 0 SOURCES: OUTFLOWS

In addition to that in direction of IRAS16293-2422, there are other peaks of H_2CO emission. They are associated with the shocks at the interface of the gas outflowing from IRAS16293 and the parental cloud gas. Highly collimated and fast outflowing gas, giving rise to « bright » shocks, are indeed a distinct propriety of Class 0 sources. The shocks of the outflow are characterized by the emission from plenty of molecules, which are not detected in cold molecular clouds. <u>SiO</u> is one of the first, and most used molecules to probe the outflows. In fact, in molecular clouds, Silicon is almost completely trapped in the dust grains, but the shocks can destroy the grain mantles, and if violent enough, also shatter the grain cores. When this occurs, Si is released into the gas, where it is readily oxidized to form SiO (following a formation route similar to that of CO). The figure on the right shows a map in the SiO 2-1 line around the Class 0 source L1448-mm. Note the outflow probed by the SiO emission: it is very collimated and possess the typical bipolar morphology.

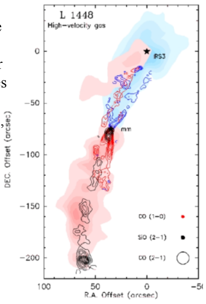

DENSITY PROFILE: Observations

<u>OBSERVATIONS: continuum emission</u>

Usually, the density profile of a protostar is derived by observations of the dust continuum emission: the Spectral Energy Distribution (SED) and the maps in the millimeter/sub-millimeter wavelength range. A typical example is shown in the figures below. By simultaneously fitting the maps at 450 and 850mm and the SED one derives the density structure of the lower right panel of the figure (dashed line), approximated by a power law. Typically, power law indexes of ~2 are found in low mass Class 0 protostars, suggesting that the "inside-out" picture is not too wrong (at least at the level of approximation possible with the single-dish observations).

The densities of protostellar envelopes range between 10^4 (at the border) to $>10^{10}$ cm^{-3} (in the inner zones).

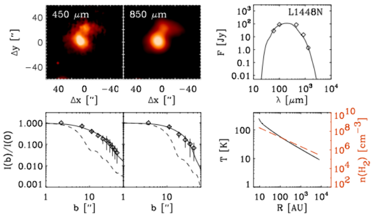

INNER ENVELOPES AND HOT CORINOS

In the inner envelopes, namely the zone of the protostellar envelopes where the dust reaches the mantle sublimation temperature (~90 K), the grain mantles sublimate injecting their components in the gas phase. It is now believed, but still far to be confirmed, that molecules like formaldehyde and methanol are synthesized on the grain surfaces, and that, when in the gas phase, these molecules start a "new" chemistry favored by the large temperature (>100 K), called *hot gas chemistry*. The result is the formation of several complex organic molecules not observed (or with a very low abundance) in cold molecular clouds: acid formic, methyl formate, cyanil vynile etc. These regions were discovered in 90s in massive star forming regions, and only more recently in low mass protostars. The have been named *hot cores* in the first case, and *hot corinos* in the second, to emphasize the different mass scale of the two classes of objects. Estimated typical densities in the hot corinos range from 10^7 to 10^9 cm^{-3}, and the radius are predicted to range between 10 to 150 AU. So far few there is only one hot corino with measured radius, though, that of IRAS16293-2422, obtained with interferometric observations (figure on the right).